

1    **Georgian bentonite clay–polymer system as a carrier for volatile  
2    oil in topical applications**

3    LIA TSIKLAURI<sup>1\*</sup>, ANA JANEZASHVILI<sup>1</sup> and MALKHAZ GETIA<sup>2</sup>

4    <sup>1</sup>*Department of Technology of Pharmaceutical Products, Biologically Active Additives &*  
5    *Cosmetics, Iovel Kutateladze Institute of Pharmacacochemistry, Tbilisi State Medical*  
6    *University, Tbilisi, Georgia and* <sup>2</sup>*Department of Pharmaceutical Analysis & Standardization,*  
7    *Iovel Kutateladze Institute of Pharmacacochemistry, Tbilisi State Medical University,*  
8    *Tbilisi, Georgia*

9    (Received 13 May, Revised 18 July, Accepted 25 November 2025)

10   *Abstract:* This study focuses on developing a polymer–clay hybrid system using  
11   a Georgian bentonite clay (Tikha-Ascane, TA) and Carbopol (CA) as a carrier  
12   for an essential oil (EO) derived from *Matricaria chamomilla* L. cultivated in  
13   East Georgia. EO was extracted *via* hydro distillation and characterized using  
14   GC–MS and FTIR techniques. The CA–TA and CA–TA–EO formulations were  
15   evaluated for key physicochemical parameters including pH, viscosity, rheology,  
16   spreadability, compatibility, moisture loss, uniformity and stability. The EO yield  
17   was 0.3 % from air-dried plant material. The main components were bisabolol  
18   oxide A (38.2 %),  $\alpha$ -bisabolol oxide B (12.91 %), (*cis*)- $\beta$ -farnesene (11.8 %),  
19    $\alpha$ -bisabolol (8.83 %), spathulenol (2.27 %), chamazulene (1.99 %), *cis*-ene-yne-  
20   dicycloether (6.51 %) and  $\beta$ -copaene (0.38 %). These results suggest that the  
21   local chamomile chemotype is rich in bisabolol oxide A. The optimized hydrogel  
22   formulation was homogeneous, stable and demonstrated favorable rheological  
23   properties, making it suitable for topical application. Chromatographic analysis  
24   confirmed the successful incorporation of the EO into the gel, which achieved  
25   an encapsulation efficiency of 58.34 %. Overall, the study confirms the compatibility  
26   of Georgian bentonite clay with the CA polymer, forming an effective  
27   matrix for volatile oil delivery in semisolid dosage forms.

28   *Keywords:* *Matricaria chamomilla*; Tikha-Ascane; essential oil–bentonite hybrid

29   **INTRODUCTION**

30   Essential oils (EOs), which are complex mixtures of volatile compounds, pos-  
31   sess numerous bioactivities and have potential applications in several industries  
32   such as the pharmaceutical, cosmetics and medicine industries. The content and  
33   chemical composition of EO are different and depend on many factors such as

\* Corresponding author E-mail: l.tsiklauri@tsmu.edu  
<https://doi.org/10.2298/JSC250513086T>

34 geographical locations, climate, the season of sampling and the method of extraction.<sup>1</sup> *Matricaria chamomilla* EO (MEO) exhibits strong anti-inflammatory, anti-35 oxidant, antimicrobial and antiviral properties and is classified as generally 36 recognized as safe (GRAS) by the FDA.<sup>2</sup> It is widely utilized to treat various 37 bacterial skin infections. However, its high volatility and instability, necessitate a 38 delivery approach that improves stability and minimizes rapid evaporation to pre-39 serve its therapeutic benefits.<sup>3-5</sup>

40 One potential solution to this issue is the encapsulation of essential oils within 41 inorganic matrices, such as clay minerals. Clays, like bentonite are widely used as 42 pharmaceutical ingredients or carriers due to their biocompatibility, interlayer 43 spacing, thermal and chemical stability. The high specific surface area, excellent 44 ion-exchange capacity, natural abundance and cost-effectiveness of bentonites 45 make them efficient carriers for volatile oils. Loading EOs into the silicate, lowers 46 the evaporation rate or slows the mass transfer of volatile components to the ext-47 ernal environment. Encapsulating various types of EOs into bentonite is an effi-48 cient way to prepare novel hybrids with antifungal and antibacterial properties. 49 Numerous studies have focused on developing EO–bentonite composites using a 50 variety of essential oils. The use of these clays as delivery systems for essential 51 oils represents a novel and promising approach.<sup>4,6</sup>

52 Over recent years, polymer–clay hybrid materials have been widely utilized 53 in drug delivery systems due to their enhanced technological properties, including 54 rheology and drug incorporation efficiency. These materials combine the advantages 55 of both components, such as swelling, water absorption and bioadhesion.<sup>7</sup> In 56 addition, polymer-based topical hydrogels are a promising drug delivery system 57 for hydrophobic compounds.<sup>8</sup>

58 In this study, we describe for the first time the synthesis of a Carbopol based 59 gel with EO obtained from *M. chamomilla* L. cultivated in Georgia and intercalated 60 in Tikha-Ascane (TA). TA is a Georgian bentonite clay preparation obtained from 61 the Askana Deposit (Ozurgeti region, Georgia) and investigated at the I. Kutatel-62 adze Institute of Pharmacocchemistry (TSMU). The biomedical and pharmaceutical 63 applications of TA have been approved by national public health authorities. Based 64 on this preparation, various dermatological formulations have been developed at 65 the Institute of Pharmacocchemistry (TSMU).<sup>9,10</sup>

## 66 EXPERIMENTAL

### 67 Preparation

68 Tikha-Ascane (TA), obtained from Georgian bentonite clay, was available at the Pharma-69 ceutical Technology Direction (I. Kutateladze Institute of Pharmacocchemistry, TSMU). Car-70 bopol 940 (CA) and methanol (catalogue no. 34860) were purchased from Sigma–Aldrich; 71 *n*-hexane was obtained from Carl Roth (Karlsruhe, Germany), and calcium chloride anhydrous 72 granules were supplied by Merck. All other solvents and chemicals obtained from commercial 73 sources were of analytical grade.

75 *Plant material*

76 *Matricaria chamomilla* L. aerial parts, cultivated in Shiraki (41°17'38" N, 46° 20'27" E,  
77 595 m asl Kiziki Floristic Region, Georgia) were collected in early June. An 120 g air-dried  
78 sample was crushed and hydrodistilled for 2 h (1:5 herb-to-water ratio) using a Clevenger-type  
79 apparatus. The resulting dark blue essential oil with a distinct aroma was stored at 4–5 °C until  
80 analysis.

81 *Qualitative and quantitative analysis of essential oil*

82 MEO constituents were analyzed using an Agilent GC-MS system (GC 7890B with  
83 5977A mass detector) equipped with an HP-5MS UI column (30 m×0.25 mm i.d.; film thickness  
84 0.25 µm). A 1 µL sample (1:100 by volume in hexane) was injected with a split ratio of 1:150,  
85 using helium as the carrier gas (1 mL/min flow, 3 mL/min purge). The oven was programmed  
86 from 140 to 215 °C at 3 °C/min, held for 4 min; injection temperature was 250 °C. MS detection  
87 was performed in TIC and SIM modes (70 eV, 40–550 amu). The relative content of each com-  
88 pound was expressed as a percentage of the total chromatographic area, based on the mean of  
89 three replicates. Identification was performed by comparing retention times and mass spectra  
90 with the NIST database.<sup>11</sup>

91 *Characterization of MEO*

92 MEO volatility was evaluated by exposing a specified quantity to the laboratory environ-  
93 ment (room temperature, 55±5 % RH), with weight loss assessed at 3, 24, 48 and 120 h.<sup>11</sup>

94 *Preparation of gel base and formulation*

95 The CA-TA gel base was prepared using 1.5 mass % CA and 2 mass % bentonite in an  
96 optimized 80:20 ratio. A 1% concentration of essential oil was selected based on prior data,  
97 yielding hydrogels with desirable rheological properties, stability and ease of application.<sup>13</sup> To  
98 prepare the gel, 2 g of bentonite was dispersed in 4 mL of deionized water, followed by incor-  
99 poration of MEO. With continuous stirring, the remaining water was gradually added and the  
100 MEO loaded clay dispersion was mixed with the 1.5 % CA gel to obtain the final hydrogel.

101 *Characterization of formulations*

102 Physical appearance and homogeneity were evaluated through visual inspection.<sup>14</sup>

103 *pH Determination*

104 The pH of all samples was determined at room temperature using a digital pH-meter  
105 (model MW150 MAX) immediately after preparation and during stability studies. The electrode  
106 was immersed into the undiluted formulations for 2 min, and the readings were recorded in  
107 triplicate.<sup>13</sup>

108 *Viscosity measurement and rheological properties*

109 A rotational viscometer (Brookfield viscometer) was used to determine the viscosity of the  
110 samples at 25±2 °C with a spindle speed of 10 rpm. The rheograms were evaluated by plotting  
111 the obtained values of shear stress versus shear rate.<sup>14</sup>

112 *Determination of spreadability*

113 The spreadability of the samples was evaluated using two sets of glass slides (20 cm×20  
114 cm). 0.5 g of the formulations were weighed and placed within a circle of 1 cm diameter pre-  
115 marked on a glass slide. A second glass plate was positioned on it, forming a sandwich arrange-  
116 ment. A weight of 500 g was placed on the upper plate for about 5 min and diameters of spread  
117 circles were assessed.

**Commented [A1]:** Please be consistent. The manuscript was written in US English. Please keep it so, do not switch to British English

118 The spreadability index ( $Si$ ) was calculated using Eq. (1); results were obtained in relation  
119 to applied mass and spreading area:<sup>15</sup>

$$120 \quad Si = d^2 \frac{\pi}{4} \quad (1)$$

121 where  $d$  is diameter (mm).

122 The spreadability factor ( $Sf$ ) was calculated as:

$$123 \quad Sf = \frac{A}{W} \quad (2)$$

124 where  $A$  is the total area (mm<sup>2</sup>) and  $W$  is the total weight (g).

125 *FTIR spectroscopy*

126 FTIR analysis was conducted to inspect the compatibility of active components with  
127 excipients. Spectra of MEO, TA and Carbopol 940 were recorded for both unloaded and loaded  
128 gel formulations in the 400–4000 cm<sup>-1</sup> range using a Jasco 600-IR spectrometer with a  
129 deuterated triglycine sulphate (DTGS) detector and KBr beam splitter. The essential oil was  
130 equilibrated at ambient temperature before analysis, and the resulting spectra were used as spec-  
131 tral fingerprints.

132 *Determination of MEO content*

133 Before GC-MS analysis, the samples were pretreated as follows: 0.1 g of CA-TA-MEO  
134 gel or 2.5 µg of MEO was mixed with methanol, filtered through a 0.45 µm filter, and 5 µL of  
135 the resulting solution was injected into the GC inlet *via* a split/splitless injector.

136 *Moisture loss*

137 The accurately weighed samples (2 g) were kept in closed desiccators containing anhydrous  
138 calcium chloride and reweighed after three days.<sup>12</sup> The percentage moisture loss was assessed  
139 using the following equation:

$$140 \quad W = 100 \frac{W_0 - W_1}{W_0} \quad (3)$$

141 where  $W_0$  is initial weight (g) and  $W_1$  is final weight (g).

142 *Optical microscopy*

143 Light microscopy was used to study the microscopic characteristics of the optimized form-  
144 ulations. Samples were placed onto a microscopic slide and uniformly spread with a coverslip.  
145 The coverslipped slides were observed at room temperature under an optical microscope (Carl  
146 Zeiss Jena CF250) at 350× magnification and photomicrographs were captured on a laboratory PC.<sup>12</sup>

147 *Centrifugation test*

148 The centrifugation test was carried out to evaluate phase separation. A 2 g sample was spun  
149 at 5000 rpm for 10 min at room temperature in a 15 mL tube.

150 *Statistical analysis*

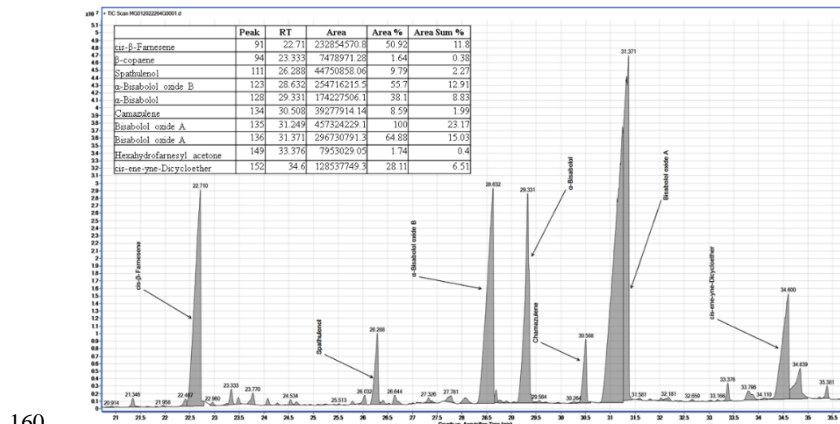
151 All analyses were performed in triplicate, and the means and standard deviations of the  
152 experimental data were calculated using Microsoft Office Excel.

153 RESULTS AND DISCUSSION

154 *Composition of essential oil*

155 The average yield of the oil from the dry chamomile aerial parts was calculated  
156 as 0.3 %. The components in the oil were examined using instrumental conditions

157 set on the GC-MS and identified using direct mass spectral comparison. The  
 158 qualitative and quantitative characteristics of MEO evaluated by the GC-MS ana-  
 159 lysis are depicted in Fig. 1.



160  
 161 Fig. 1. GC-MS profile of essential oil extracted from dried chamomile aerial parts.

162 The major constituents were found to be bisabolol oxide A (38.2 %),  $\alpha$ -bisab-  
 163 ol oxide B (12.91 %), (cis)- $\beta$ -farnesene (11.8 %),  $\alpha$ -bisabolol (8.83 %), spathulenol  
 164 (2.27 %), chamazulene (1.99 %), cis-ene-yne-dicycloether (6.51 %) and  $\beta$ -copaene  
 165 (0.38 %). These findings classify the East Georgian chamomile oil as a bisabolol  
 166 oxide A chemotype. Bisabolol oxide A, a sesquiterpenoid, is recognized for its  
 167 broad spectrum of biological activities, including anti-herpetic, antipruritic, anti-  
 168 microbial, cytotoxic and antileishmanial effects.<sup>16</sup>

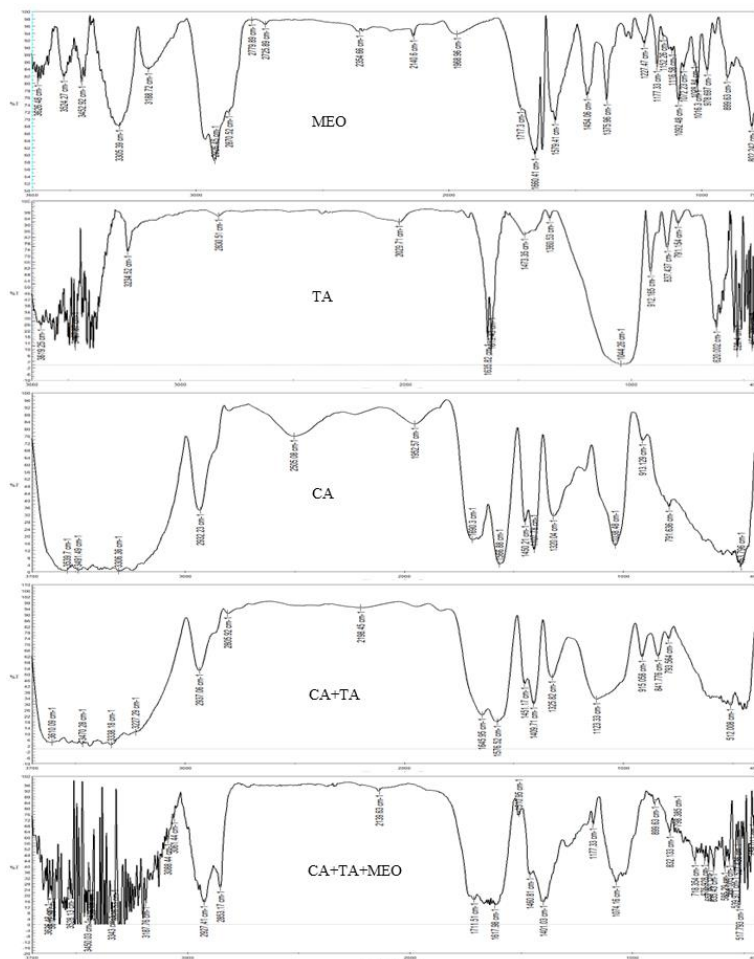
169 *FTIR analysis*

170 Essential oils are complex mixtures comprising volatile and aromatic com-  
 171 pounds, often associated with a wide range of functional groups. In the present  
 172 study, MEO was found to contain ethers, amines, carboxylic acid, aromatics,  
 173 alkanes, aldehyde carbonyl, aldehyde and alcohols (Fig. 2). The assignments of  
 174 corresponding functional groups were achieved by using frequency data available  
 175 in the literature.<sup>17-19</sup>

176 The FTIR spectrum of MEO showed characteristic bands corresponding to its  
 177 main components. A broad band at 3200–3600  $\text{cm}^{-1}$  indicated O–H stretching  
 178 from alcohols and phenols.<sup>18,19</sup> A peak at  $\sim 2926.45 \text{ cm}^{-1}$  was assigned to C–H  
 179 stretching in alkanes.<sup>17,20</sup> The band at  $\sim 1717 \text{ cm}^{-1}$  was assigned to the C=O stretch

**Commented [A2]:** Please check if the meaning has changed.

180 of matricin, with low intensity suggesting its conversion to chamazulene and car-  
 181 boxylic derivatives.<sup>21,22</sup> Peaks at  $\sim$ 1631 and 1660.41  $\text{cm}^{-1}$  indicated C=C stretching  
 182 of alkenes (*e.g.*, farnesene), while that at  $\sim$ 1579  $\text{cm}^{-1}$  was assigned to aromatic C=C  
 183 vibration.<sup>19,27,22-25</sup>



184

185

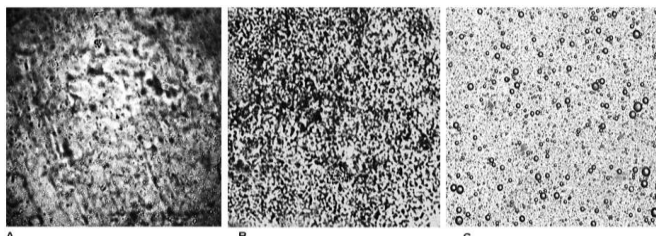
Fig. 2. FTIR spectra of the tested samples.

186 Bands at  $\sim$ 1454 and 1375  $\text{cm}^{-1}$  reflected  $\text{CH}_2$  and  $\text{CH}_3$  deformation, possibly  
 187 from  $\alpha$ -bisabolol and its oxides.<sup>19,22-25</sup> A peak around 1227  $\text{cm}^{-1}$  corresponded  
 188 to esters and phenolic C–O stretching.<sup>24</sup> Bands between 1177–1016.3  $\text{cm}^{-1}$   
 189 corresponded to alcohol or ether C–O stretches, including signals from *cis/trans*-  
 190 -en-yne-dicycloether.<sup>23,24</sup> Peaks in the 1092–899  $\text{cm}^{-1}$  range matched  $\alpha$ -bisabolol  
 191 (tertiary alcohols) while the peak at  $\sim$ 978  $\text{cm}^{-1}$  indicated methylene or aromatic in-  
 192 plane bending.<sup>19,21,23,25</sup> Finally, peaks between 899–802  $\text{cm}^{-1}$  were attributed to  
 193 out-of-plane aromatic C–H bending.<sup>21,24</sup>

194 The volatilization test revealed that free MEO exhibited weight losses of 20.3,  
 195 50.8, 53.0 and 54.7 % after 3, 24, 48 and 120 h, respectively, confirming its high  
 196 volatility and highlighting the limitations of conventional encapsulation strategies.  
 197 Bentonite clays, due to their unique layered structure, can effectively interact with  
 198 essential oil molecules.<sup>26</sup> In this study, the interlayer space of bentonite was acti-  
 199 vated in water, followed by mechanical intercalation of MEO. This approach  
 200 enabled successful incorporation of oil into the clay framework, as confirmed by  
 201 volatilization assays and light microscopy (Fig. 3). Encapsulation of MEO within  
 202 the bentonite matrix reduced its volatilization by 65.26, 65.32, 68.68 and 68.94 %  
 203 at 3, 24, 48 and 120 h, respectively, compared to the free, unencapsulated oil,  
 204 thereby demonstrating enhanced stability and decreased volatility.

205 As visualized in Fig. 3C, dark, spherical droplets of MEO are distributed  
 206 throughout the well-dispersed carbopol–bentonite matrix, and the network struc-  
 207 ture of the hydrogel is capable of protecting the essential oil from evaporating.  
 208 After addition of Matricaria chamomilla EO, the structure of CA-TA system  
 209 changed, showing a fibrous-like network, which can be expected as a result of the  
 210 interactions of matrix components with MEO compounds.

211 Microscopic analysis of the formulations (Fig. 3) showed that the CA-TA-  
 212 –MEO system exhibits a nearly monodisperse microstructure with small, homo-  
 213 geneously dispersed oil droplets. Droplet size is known to influence the physico-  
 214 chemical stability and mechanical properties of emulsion gels. Generally, smaller  
 215 droplets with a narrow size distribution improve physical stability.<sup>27</sup>



216  
 217 Fig. 3. Light microphotographs of tested samples. A) TA; B) CA-TA matrix;  
 218 C) MEO loaded hydrogel (1 mass %).

219 The optical microscopy images of the hybrid microstructure of bentonite  
 220 modified carbopol gel (Fig. 3B) showed a non-uniform texture. The existence of  
 221 non-homogeneous areas confirms the interaction between TA and the polymer  
 222 chains, providing appropriate interconnected architecture in the system. Also, Fig.  
 223 3A shows the heterogeneous texture for the aqueous TA suspension (2 mass %),  
 224 typical of bentonite gels due to the clay platelets' tendency to form a structured  
 225 network.

226 The outcome of this study showed that TA clay and the CA polymer are  
 227 compatible with one another, leading to the formation of stable [TA+CA] matrix  
 228 suitable for the incorporation of essential oil.

229 *Characterization of formulations*

230 Prepared gels were found to be blue in color, homogeneous and visually  
 231 acceptable. The gel has the characteristic odor of the essential oil of *Matricaria*  
 232 *chamomilla*.

**Commented [A3]:** Please check if the meaning has changed.

233 *pH Determination*

234 The pH values of the prepared formulations are given in Table I.

235 The results suggest that CA-TA-MEO gel is skin-compatible and suitable for  
 236 topical use.<sup>28</sup> The initial pH of bentonite suspensions ranged from 8.6 to 9.0,  
 237 whereas the pH of CA-TA formulations remained between 6.5 and 6.71, and that  
 238 of carbopol gels ranged from 6.47 to 6.63.

239 TABLE I. pH, spreadability and moisture loss of the formulations; SD: standard deviation, n = 3

Sample	pH (mean $\pm$ SD)	Sf / mm <sup>2</sup> g <sup>-1</sup> (mean $\pm$ SD)	w / %
2 % TA	8.84 $\pm$ 0.12	—	—
1.5 % CA 940	6.53 $\pm$ 0.06	6.89 $\pm$ 0.52	3.33 $\pm$ 0.05
CA-TA	6.58 $\pm$ 0.09	6.39 $\pm$ 0.52	4.59 $\pm$ 0.04
CA-TA-MEO	6.57 $\pm$ 0.04	7.16 $\pm$ 0.33	3.76 $\pm$ 0.03

240 *Viscosity measurement and determination of rheological properties*

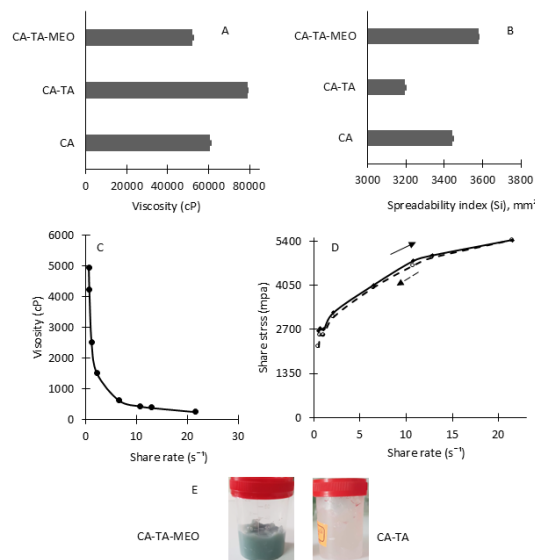
241 The viscosity and rheology of semisolid formulations influence their applica-  
 242 tion behavior and spreadability. The highest viscosity was observed for the ben-  
 243 tonite-modified carbopol gel (78,933 cP), while the MEO gel possessed the lowest  
 244 viscosity (52,267 cP). Bentonite increased the viscosity, whereas MEO incorporation  
 245 into the CA-TA matrix resulted in a decrease (Fig. 4A).

246 The viscosity of the CA-TA-MEO gel was assessed at different speed rates;  
 247 the rheological profile of formulation demonstrated a shear-thinning behavior,  
 248 where viscosity decreased with increasing shear rate – indicative of a non-Newtonian,  
 249 pseudoplastic system (Fig. 4C and D).

250 This property is advantageous for topical applications, as it enables reduced  
 251 resistance during spreading while maintaining structural integrity at rest. The MEO

**Commented [A4]:** Please check if the meaning has changed.

252 gel also displayed an insignificant hysteresis loop, indicating negligible thixotropic  
 253 properties, a typical feature of carbomer-based gels. Such behavior enhances applica-  
 254 tion consistency and storage stability.<sup>29,30</sup>



255  
 256 Fig. 4. Evaluation of physical properties and rheological behavior of samples: A) viscosity,  
 257 B) spreadability measurements, C) viscosity at different shear rates, D) flow profile of  
 258 CA-TA-EO gel and E) visual presentation of CA-TA and CA-TA-EO formulations.

#### 259 *Determination of spreadability*

260 The effectiveness of topical formulations relies on uniform spreading to  
 261 ensure accurate dosing and ease of application. Spreadability, a key parameter for  
 262 semisolid dosage forms, is inversely related to viscosity – a decrease in viscosity  
 263 leads to improved spreadability. A good spreadability for gel formulations is con-  
 264 sidered to lie within the 2500–4900 mm<sup>2</sup> range.<sup>31</sup> As shown in fig. 4B and Table I,  
 265 the CA-TA-MEO gel, with the lowest viscosity, exhibited the highest spread-  
 266 ability index (3579.21 mm<sup>2</sup>) and factor, indicating favorable spreading properties  
 267 suitable for topical use.

#### 268 *FTIR analysis of samples*

269 Infrared spectra of the optimized formulation confirmed the absence of incom-  
 270 patibility among the components. FTIR analysis also contributed to verify the pre-

sence of MEO within the TA-CA gel matrix. Similar to the spectra of CA and TA-CA, the TA-CA-MEO formulation exhibited the characteristic absorption bands of pure CA and TA-CA. The encapsulation of the essential oil by the TA-CA matrix could be evidenced by the appearance of additional specific bands corresponding to components present in MEO (Fig. 2). Bands at 2927.41 and 2853.17  $\text{cm}^{-1}$  characteristic of the C-H stretching vibrations of alkanes, were displayed only in the TA-CA-MEO gel. Moreover, absorption peaks at  $\sim$ 1700, 1177 and 899  $\text{cm}^{-1}$  in Fig. 2 corresponded to the C=O, stretching of aldehydes, C–O stretching of ethers, and C–H bending of aromatic compounds, respectively.<sup>22</sup>

In the infrared spectrum of Carbopol 940 the characteristic peaks of O–H stretch at 3306.36  $\text{cm}^{-1}$  and C–O stretch at 1407.78  $\text{cm}^{-1}$  were observed; the peak at 2932.23  $\text{cm}^{-1}$  represents  $\text{CH}_2$  stretching, whereas the 1450.21  $\text{cm}^{-1}$  peak shows the presence of the acrylate back bone (Fig. 2). It is also noted that similar peaks were found in the spectra of the hybrid matrix and TA-CA-MEO gel, confirming the structural integrity of the polymer within the formulation.<sup>32</sup>

The bonds at 3467.87 and 3620.21  $\text{cm}^{-1}$  in the spectrum of the original TA are characteristic of Si–OH and Al–OH stretching vibrations in bentonite. A sharp peak at 1044.26  $\text{cm}^{-1}$  is associated with Si–O stretching vibration. Compared to the original bentonite, the Si–O absorption peak shifts to a lower wavenumber in the hybrid matrix spectrum, while in the TA-CA-MEO formulation, it moves to a higher wavenumber with reduced intensity—indicating gel network formation. The small peak at 912.16  $\text{cm}^{-1}$  is attributed to the bending vibration of –OH in Al–Al–OH, a characteristic feature of bentonite.<sup>33</sup> As shown in Fig. 2, the peak at 791.15  $\text{cm}^{-1}$  represents Al–Mg–OH vibrations, while the peak at 620.00  $\text{cm}^{-1}$  corresponds to Mg–O–Si or Fe–O–Si groups. Peaks at 528.4 and 461.38  $\text{cm}^{-1}$  are related to Al–O and Mg–O, respectively.<sup>34</sup>

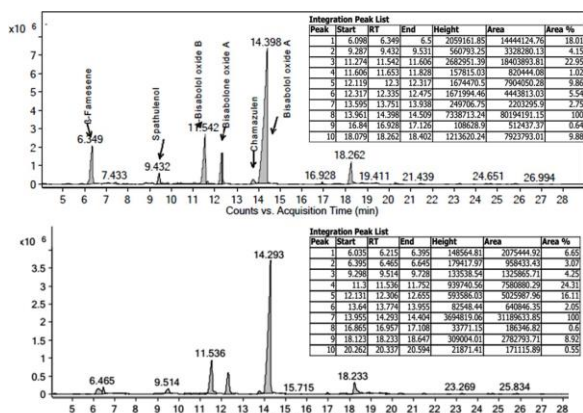
FTIR spectral analysis of the essential oil, bentonite, and Carbopol 940 confirmed that the characteristic peaks of the essential oil were preserved in the gel formulation, indicating no significant interactions among the formulation components.

### 301 *Determination of MEO content*

302 GC–MS analysis revealed comparable chromatographic profiles across the  
303 tested formulations, verifying the presence of characteristic constituents of *M.*  
304 *chamomilla* EO (Fig. 5). The MEO content in the CA–TA–MEO gel assessed as a  
305 function of the initial EO loading, averaged 58.34%.

306 Despite the simplicity of the formulation process, a reduction in MEO content  
307 was observed, likely due to volatility or process-related factors that require further  
308 investigation. To date, no studies have reported the encapsulation efficiency of *M.*  
309 *chamomilla* EO in bentonite-based gels or the CA–TA system specifically. How-  
310 ever, *EE* values for other essential oils range from 47.69 to 57.8 %, depending on

311 formulation variables, polymer type and analytical methods.<sup>35</sup> The *EE* observed  
 312 here aligns with these findings, indicating that the CA–TA system forms a stable,  
 313 well-structured matrix capable of effectively encapsulating MEO.



314  
 315 Fig. 5. GC-MS chromatograms of pure MEO (A) and CA–TA–MAO gel formulation (B).

### 316 *Moisture loss*

317 Water content is fundamental for hydrogel integrity and solubility, as evapo-  
 318 ration significantly alters hydrogel properties.<sup>36</sup> Moisture loss analysis (Table I)  
 319 showed that CA–TA–MEO exhibited the lowest loss, which is advantageous for  
 320 preserving the gel's physical properties during storage. Centrifugation tests further  
 321 confirmed the physical stability, with no phase separation observed.

### CONCLUSION

323 *Matricaria chamomilla* essential oil (MEO) demonstrates a wide range of phar-  
 324 macological activities; however, its high volatility and chemical instability hinder  
 325 its direct application in topical formulations. Furthermore, MEOs compositions  
 326 can vary significantly depending on factors such as geographical origin, climate,  
 327 harvesting season and extraction method.

328 This study developed and evaluated a Georgian bentonite clay (TA)–polymer  
 329 system for topical delivery of volatile oils. The gel was formulated with Carbopol  
 330 (CA) and an MEO–TA hybrid. Analysis confirmed that East Georgian chamomile  
 331 cultivars belong to the bisabolol oxide A chemotype, with major constituents inc-  
 332 luding bisabolol oxide A,  $\alpha$ -bisabolol oxide B, (*cis*)- $\beta$ -farnesene,  $\alpha$ -bisabolol, spat-  
 333 hulenol, chamazulene, *cis*-ene-yne-dicycloether and  $\beta$ -copaene.

334 To minimize evaporation and slow the mass transfer of volatile components,  
 335 an MEO–TA hybrid was incorporated into an 1.5 % Carbopol gel. The resulting  
 336 MEO–TA–CA formulations satisfied key requirements for semisolid dosage  
 337 forms, including uniformity, physical stability and suitable rheological behavior.  
 338 EO droplets were well-incorporated and evenly distributed into the matrix. FTIR  
 339 analysis confirmed the preservation of MEO's characteristic peaks, indicating the  
 340 absence of undesirable interactions between the formulation components.

341 The prepared gel showed a significant encapsulation capacity for MEO, rich  
 342 in bisabolol oxide A – a bioactive compound with anti-herpes, antipruritic and  
 343 antimicrobial properties – highlighting the potential of Georgian bentonite clay–  
 344 polymer systems for topical delivery of volatile oils.

## ИЗВОД

ХИБРИДНИ СИСТЕМ ГРУЗИЈСКИ БЕНТОНИТ–ПОЛИМЕР КАО НОСАЧ ЗА ЕТЕРИЧНО  
УЉЕ У ТОПИКАЛНИМ ПРИМЕНАМАLIA TSIKLAURI<sup>1</sup>, ANA JANEZASHVILI<sup>1</sup> и MALKHAZ GETIA<sup>2</sup>

349 <sup>1</sup>Department of Technology of Pharmaceutical Products, Biologically Active Additives & Cosmetics, Iovel  
 350 Kutateladze Institute of Pharmacacochemistry, Tbilisi State Medical University, Tbilisi, Georgia и <sup>2</sup>Department  
 351 of Pharmaceutical Analysis & Standardization, Iovel Kutateladze Institute of Pharmacacochemistry, Tbilisi  
 352 State Medical University, Tbilisi, Georgia

353 Циљ овог рада је био развој хибридног система полимер–глина коришћењем грузиј-  
 354 ског бентонита (*Tikha-Ascane*, TA) и полимера *Carbopol* (CA) као носача за етерично уље  
 355 (EO) добијено из камилице (*Matricaria chamomilla L.*) која је узгајана у Источној Грузији.  
 356 EO је екстраговано хидролизацијом и окарактерисано применом GC–MS и FTIR тех-  
 357 ника. Одређени су основни физичко–хемијски параметри формулација CA–TA и CA–TA–  
 358 –EO, као што су pH, вискозност, реологија, распостирање, компатибилност, губитак  
 359 влаге и стабилност. Принос EO је био 0,3 % из биљног материјала који је сушен на ваздуху.  
 360 Главне компоненте су бисаболол-оксид А (38,2 %),  $\alpha$ -бисаболол-оксид В (12,91 %), (*cis*)-  
 361 – $\beta$ -фарнесен (11,8 %),  $\alpha$ -бисаболол (8,83 %), спатуленол (2,27 %), камазулен (1,99 %), *cis*-  
 362 –ен-ин-дициклоетар (6,51 %) и  $\beta$ -копаен (0,38 %). Ови резултати су показали да је локална  
 363 камилица богата бисаболол-оксидом А. Оптимизована хидрогел формулација је била  
 364 хомогена, стабилна, са добрым реолошким својствима, погодна за актуелне примене.  
 365 Хроматографска анализа је потврдила успешно инкорпорирање EO у гел, са ефикасно-  
 366 шћу имобилизације од 58,34 %. Генерално, ова испитивања су показала да је грузијски  
 367 бентонит компатибилан са CA полимером и да формира ефикасну матрицу за испоруку  
 368 етеричног уља у получуврстом облику.

369 (Примљено 13. маја, ревидирано 18. јула, прихваћено 25. новембра 2025)

## REFERENCES

370 1. D. P. de Sousa, R. O. S. Damasceno, R. Amorati, H. A. Elshabrawy, R. D. de Castro, D.  
 371 P. Bezerra, V. R. V. Nunes, R. C. Gomes, T. C. Lima, *Biomolecules* **13** (2023) 1144  
 372 (<https://doi.org/10.3390/biom13071144>)  
 373 2. A. El Miyaoui, J. C. G. Esteves da Silva, S. Charfi, M. E. Candela Castillo, A. Lamarti,  
 374 M. B. Arnao, *Life* **12** (2024) 479 (<https://doi.org/10.3390/life12040479>)

376 3. G. Ren, G. Ke, R. Huang, Q. Pu, J. Zhao, Q. Zheng, M. Yang, *Sci. Rep.* **12** (2022) 8153  
377 (<https://doi.org/10.1038/s41598-022-11692-w>)

378 4. J. N. Saucedo-Zuñiga, S. Sánchez-Valdes, E. Ramírez-Vargas, L. Guillen, L. F. Ramos-  
379 -deValle, A. Graciano-Verdugo, J. A. Uribe-Calderón, M. Valera-Zaragoza, T. Lozano-  
380 -Ramírez, J. A. Rodríguez-González, J. J. Borjas-Ramos, J. D. Zuluaga-Parra,  
381 *Microporous Mesoporous Mater.* **316** (2021) 110882  
382 (<https://doi.org/10.1016/j.micromeso.2021.110882>)

383 5. L. H. Oliveira, I. S. de Lima, E. R. S. da Neta, S. G. de Lima, P. Trigueiro, J. A. Osajima,  
384 E. C. da Silva-Filho, M. Jaber, M. G. Fonseca, *Appl. Clay Sci.* **245** (2023) 107158  
385 (<https://doi.org/10.1016/j.clay.2023.107158>)

386 6. A. Giannakas, I. Tsagkalias, D. S. Achilias, A. Ladavos, *Appl. Clay Sci.* **146** (2017) 362  
387 (<https://doi.org/10.1016/j.clay.2017.06.018>)

388 7. F. Sorouri, P. Azimzadeh Asiabi, P. Hosseini, A. Ramazani, S. Kiani, T. Akbari, M.  
389 Sharifzadeh, M. Shakoori, A. Foroumadi, L. Firoozpour, M. Amin, M. Khoobi, *Polym.*  
390 *Bull.* **80** (2023) 5101 (<https://doi.org/10.1007/s00289-022-04306-y>)

391 8. M. Chelu, *Gels* **10** (2024) 636 (<https://doi.org/10.3390/gels10100636>)

392 9. I. G. Kutateladze, *Tikha-Ascane for medical purpose*, Gruzmedgiz, Tbilisi, 1955, p. 40

393 10. L. Tsiklauri, I. Dadeshidze, G. Tsagareishvili, *Bull. Georgian Natl. Acad. Sci.* **150** (1994)  
394 262 (ISSN 0132-1447)

395 11. N. Tsivelika, E. Sarrou, K. Gusheva, C. Pankou, T. Koutsos, P. Chatzopoulou, A.  
396 Mavromatis, *Biochem. Syst. Ecol.* **80** (2018) 21  
397 (<https://doi.org/10.1016/j.bse.2018.06.001>)

398 12. R. Ensandoost, H. Izadi-Vasafi, H. Adelnia, *J. Macromol. Sci. Phys.* **61** (2021) 225  
399 (<https://doi.org/10.1080/00222348.2021.1999043>)

400 13. N. Ullah, A. Amin, A. Farid, S. Selim, S. A. Rashid, M. I. Aziz, S. H. Kamran, M. A.  
401 Khan, N. Rahim Khan, S. Mashal, M. M. Hasan, *Gels* **9** (2023) 252  
402 (<https://doi.org/10.3390/gels9030252>)

403 14. M. Singh, J. Kanoujia, P. Parashar, M. Arya, C. B. Tripathi, V. R. Sinha, S. K. Saraf, S.  
404 A. Saraf, *Drug Deliv. Transl. Res.* **8** (2018) 591 (<https://doi.org/10.1007/s13346-018-0489-5>)

405 15. B. Siddiqui, A. U. Rehman, I. U. Haq, N. M. Ahmad, N. Ahmed, *J. Microencapsul.* **37**  
406 (2020) 595 (<https://doi.org/10.1080/02652048.2020.1829140>)

407 16. I. Ikeda-Ogata, K. Yamasaki, K. Yokomizo, T. Ikeda, H. Seo, *Curr. Top. Phytochem.* **17**  
408 (2021) 63  
409 ([http://www.researchtrends.net/tia/article\\_pdf.asp?in=0&vn=17&tid=24&aid=6834](http://www.researchtrends.net/tia/article_pdf.asp?in=0&vn=17&tid=24&aid=6834))

410 17. Ö. Süfer, F. Bozok, *J. Therm. Anal. Calorim.* **140** (2020) 253  
411 (<https://doi.org/10.1007/s10973-019-08829-x>)

412 18. S. Agatonovic-Kustrin, P. Ristivojevic, V. Gegechkori, T. M. Litvinova, D. W. Morton,  
413 *Appl. Sci.* **10** (2020) 7294 (<https://doi.org/10.3390/app10207294>)

414 19. L. Ciko, A. Andoni, F. Ylli, E. Plaku, K. Taraj, *J. Int. Environ. Appl. Sci.* **11** (2016) 154  
415 (<https://dergipark.org.tr/tr/download/article-file/571496>)

416 20. M. I. Morar, F. Fetean, A. M. Rotar, M. Nagy, C. A. Semeniuc, *Bull. UASVM Food Sci.*  
417 *Technol.* **74** (2017) 37 (<https://doi.org/10.15835/buasvmcn-fst:12634>)

418 21. H. Schulz, M. Baranska, H. H. Belz, P. Rösch, M. A. Strehle, J. Popp, *Vib. Spectrosc.* **35**  
419 (2004) 81 (<https://doi.org/10.1016/j.vibspec.2003.12.014>)

420

421 22. K. Taraj, I. Malollari, A. Andoni, L. Ciko, P. Lazo, F. Ylli, A. Smeni, A. Como, *J.  
422 Environ. Prot. Ecol.* **18** (2017) 117  
(<https://scibulcom.net/en/article/Sut8GqESZGR7LPJJIKEw>)

423 23. M. D. Berechet, E. Manaila, M. D. Stelescu, G. T. Craciun, *Rev. Chim.* **68** (2017) 2787  
(<https://doi.org/10.37358/RC.17.12.5979>)

424 24. Y. Q. Li, D. X. Kong, H. Wu, *Ind. Crops Prod.* **41** (2013) 269  
(<https://doi.org/10.1016/j.indcrop.2012.04.056>)

425 25. A. Andoni, F. Ylli, P. Lazo, K. Taraj, A. Como, *BSHN (UT)* **24** (2017) 152  
([https://api.fshn.edu.al/uploads/1\\_Andoni\\_et\\_al\\_rreg\\_3bb9acf7ff.pdf](https://api.fshn.edu.al/uploads/1_Andoni_et_al_rreg_3bb9acf7ff.pdf))

426 26. L. H. de Oliveira, P. Trigueiro, J. S. N. Souza, M. S. de Carvalho, J. A. Osajima, E. C. da  
427 Silva-Filho, M. G. Fonseca, *Colloids Surfaces, B* **209** (2022) 112186  
(<https://doi.org/10.1016/j.colsurfb.2021.112186>)

428 27. J. Santos, L. A. Trujillo-Cayado, F. Carrillo, M. L. López-Castejón, M. C. Alfaro-Rod-  
429 ríguez, *Polymers* **14** (2022) 2195 (<https://doi.org/10.3390/polym14112195>)

430 28. X. Nqoro, S. A. Adeyemi, P. Ubanako, D. T. Ndintehal, P. Kumar, Y. E. Choonara, B. A.  
431 Aderibigbe, *Polym. Bull.* **81** (2024) 3459 (<https://doi.org/10.1007/s00289-023-04879-2>)

432 29. M. F. A. Khan, A. Ur Rehman, H. Howari, A. Alhodaib, F. Ullah, Z. ul Mustafa, A.  
433 Elaissari, N. Ahmed, *Gels* **8** (2022) 277 (<https://doi.org/10.3390/gels8050277>)

434 30. Y. Maslii, O. Ruban, G. Kasparaviciene, Z. Kalveniene, A. Materienko, L. Ivanauskas,  
435 A. Mazurkeviciute, D. M. Kopustinskiene, J. Bernatoniene, *Molecules* **25** (2020) 5018  
(<https://doi.org/10.3390/molecules2515018>)

436 31. M. X. Chen, K. S. Alexander, G. Baki, *J. Pharm. (Cairo)* **2016** (2016) 5754349  
(<https://doi.org/10.1155/2016/5754349>)

437 32. J. El Karkouri, M. Bouhrim, O. M. Al Kamaly, H. Mechhate, A. Kchibale, I. Adadi, S.  
438 Amine, S. Alaoui Ismaili, T. Zair, *Plants* **10** (2021) 2068  
(<https://doi.org/10.3390/plants10102068>)

439 33. M. G. Martins, D. O. A. Martins, B. L. C. de Carvalho, L. A. Mercante, S. Soriano, M.  
440 Andruh, M. D. Vieira, M. G. F. Vaz, *J. Solid State Chem.* **228** (2015) 99  
(<https://doi.org/10.1016/j.jssc.2015.04.024>)

441 34. M. Edraki, D. Zaarei, *J. Nanoanalysis* **5** (2018) 26  
(<https://sanad.iau.ir/fa/Journal/jnanoanalysis/DownloadFile/988806>)

442 35. K. G. Torres, R. R. Almeida, S. Y. de Carvalho, J. F. Haddad, A. A. Leitao, L. G.  
443 Guimaraes, *Mater. Today Commun.* **24** (2020) 101252  
(<https://doi.org/10.1016/j.mtcomm.2020.101252>)

444 36. A. Vesković, D. Nakarada, A. Popović Bijelić, *Polym. Test.* **98** (2021) 107187  
(<https://doi.org/10.1016/j.polymertesting.2021.107187>).